LUMINESCENCE ENHANCEMENT OF OLED PERFORMANCE BY DOPING COLLOIDAL MAGNETIC Fe$_3$O$_4$ NANOPARTICLES

Mahmut Kus[1, 2] *, Faruk Ozel[1, 2], Nurhan M. Varal[2, 4], and Mustafa Ersoz[2, 3]

[1]Department of Chemical Engineering, Selcuk University, Konya 42075, Turkey

[2]Advanced Technology Research and Application Center, Selcuk University, Konya 42075, Turkey

[3]Department of Chemistry, Selcuk University, Konya 42075, Turkey

[4]Department of Physics, Selcuk University, Konya 42075, Turkey

Abstract—We report synthesis of magnetic Fe$_3$O$_4$ nanoparticles (MNPs) based on two phase method and their application in organic light-emitting devices (OLEDs) as blend with emissive Polyfluorene (PFO) matrix. Two phase method allows to successively synthesizing oleic acid capped MPNs with 5–10 nm particle size. Colloidal MNPs can be easily mixed with emissive polymer solutions to obtain a blend for OLED application. The electroluminescence efficiency increases by doping with MNPs into emissive layer. Different dopant concentrations varied from 0,4% to 2% were monitored. It was observed that the electroluminescence increases up to 1% w/v doping ratio. The luminance of OLEDs increased from 15.000 cd/m^2 to 24.000 cd/m^2 in comparison pristine device with 1% MNP doped device.

1. INTRODUCTION

Over the last decade magnetic materials have been extensively investigated due to their potential use in electronics [1–3]. Fe$_3$O$_4$ magnetic nanoparticles (MNPs) become soluble by capping with some surfactants such as oleylamine or oleic acid. Thus, surfactant capped MNPs can be easily dissolved to give colloidal solutions in organics or water. There have been many reports on synthesis of colloidal

MNPs [4–7]. However, most of routes to synthesize colloidal MNPs in organic solvents require reaching high temperatures between 200–260°C during synthesis [6–8]. High temperature synthesis are mostly carried out in organic surfactants such as oleylamine, hexadecylamine or oleic acid. On the other hand some routes for low temperature synthesis in water have also been reported [9–12]. Two phase route, firstly reported by Pan et al. is a facile method to synthesize colloidal nanoparticles [13]. There are several reports on synthesis of quantum nanocrystals based on two phase route but it is scarce for MNPs [14, 15]. Since the formation and growth of nanocrystals occurs at interface and formed nanocrystals stay in organic phase, two phase method allows obtaining highly pure crystals by a simple precipitation. In addition, two phase method leads homogenous growth and narrow particle size distribution at low reaction temperature. However, other methods require high temperature synthesis leading very fast particle growth that results in broad size distribution. Moreover, well known synthetic methods, that are carried out in one phase, require several purification process to obtain pure crystals. Facile and controllable synthesis of MNPs supply a great advantage for device fabrication based on solution proceed.

The effect of magnetic field on the performance of PLEDs (or OLEDs) has been investigated by many groups to enhance the emission intensity of organic or polymer light emitting diodes [16–20]. It is well known that PLEDs have been attracting a great attention due to their advantages in emission in a wide visible region and for applications to flat-panels or as light sources for optical signal circuits or other applications [21]. Although significant progress has been achieved on the performance of PLEDs, further improvement is still needed such as stability, brightness and lifetime for their commercial applications [22]. Polyuorene derivatives (PFs) are among the most promising emitter materials for PLEDs because of their high photoluminescence (PL) efficiencies, their blue to blue-green emission spectra, and their potential for synthetic modification [23–28]. However, the performance of PFs in PLEDs has been limited by tendencies to form aggregates, excimers, or carbonyl defects, resulting in less-efficient emission and unreliable emission characteristics, especially undesired long-wavelength bands [23–32].

Kalinowski et al. reported that the application of magnetic field of 500 mT lead to increase the current ow as well as light output by 3% in Alq$_3$ based OLEDs [16, 33]. On the other hand, the change in resistance more than 10% was achieved in polyuorene (PFO) devices at room temperature under weak magnetic field of 10 mT [33, 34]. The effect of CoPt ferromagnetic nanowires on the exciton formation

in poly (2-methoxy, 5-(2-ethylhexiloxy)1, 4-phenylenevinylene) (MEH-PPV) and iridium complex Ir(ppy)3 was investigated by Hu et al. [35]. They reported that the spin-polarized holes transferred from CoPt nanowires to the polymer and iridium complex enhance the singlet to triplet ratio in the presence of magnetic field [35]. Sun et al. observed that the quantum efficiency increased from 27% to 32% by doping 0.1 wt% CoFe magnetic nanoparticles into polymer matrix [36]. The doping of CoFe in MEH-PPV matrix reduces the hole mobility from 1×10^{-5} to $6 \times 10^{-6} \, \mathrm{cm^2 V^{-1} s^{-1}}$ by introducing new trap sites causing their net density increase from 1×10^{18} to $2.1 \times 10^{18} \, \mathrm{cm^3}$, which is likely to result in balanced injection and efficient recombination of charge carriers to improve the performance of polymer light emitting diodes [37]. Zhang et al. investigated the effect of Fe_3O_4 MNPs as a buffer layer on the ITO surface. The luminance and the current density are significantly enhanced by using the Fe_3O_4/ITO anode, as well as the turn-on voltage is reduced by 1.5 V compared to the devices without the buffer [22]. Besides application in PLEDS or OLEDs, the effect of magnetic nanoparticles on organic solar cells has been also investigated by Zhang et al.. The increase in efficiency by 18% at the optimum Fe_3O_4 NPs doping ratio of 1% was observed in Fe_3O_4 NPs doped P3HT:PCBM solar cell. This enhancement is primarily due to the increase of Jsc (14% enhancement), which is attributed to the magnetic field effect originated from the superparamagnetism of Fe_3O_4 NPs, resulting in the increase of the population of triplet excitons [38].

In this study, we reported synthesis of Fe_3O_4 MNPs based on two phase route and demonstrated the luminescence enhancement of MNP doped PLEDs. As mentioned above the application of two phase route to synthesize colloidal MNPs is scarce [14, 15]. We aimed to contribute the facile and low temperature synthesis of MNPs. On the other hand we have not been reached any report about application of colloidal MNPs as a dopant to improve the performance of Polyuorene based PLED devices.

2. EXPERIMENTAL

2.1. Materials

$FeCl_2 \cdot 4H_2O$ (Merck), $FeCl_3 \cdot 6H_2O$ (Merck), oleic acid (Sigma-Aldrich), Polyflourene (Sigma-Aldrich), PEDOT:PSS (Clevios PVP AI4083, H. C. Stark) and ITO coated glasses (KINTEC Co.) with a sheet resistance between 10–$12 \, \Omega \mathrm{square}^{-1}$ were purchased from different suppliers as shown in parenthesis. All solvents such as toluene, chlorobenzene, etc. were HPLC grade and supplied from Merck-Germany.

2.2. Synthesis of Colloidal Magnetic Nanoparticles

3.5 grams of FeCl$_3$·6H$_2$O and 2 grams of FeCl$_2$·4H$_2$O are dissolved in
60 ml deionized water. The mixture is mixed and stirred under nitrogen
flow for 5 min. 2.5 ml of oleic acid is dissolved in 80 ml of toluene and
this solution is added to aqueous solution. Then, 20 ml of ammonium
hydroxide (25%) solution is added to mixture. A black suspension
is observed by adding ammonium hydroxide. The temperature is
adjusted to 70°C and mixture is stirred under nitrogene atmosphere for
1 h. Then, the solution is allowed to cool down to room temperature.
After the separation of water and toluene phase, 40 ml of isopropanol is
added to toluene solution to participate MNPs. After filtration, MNPs
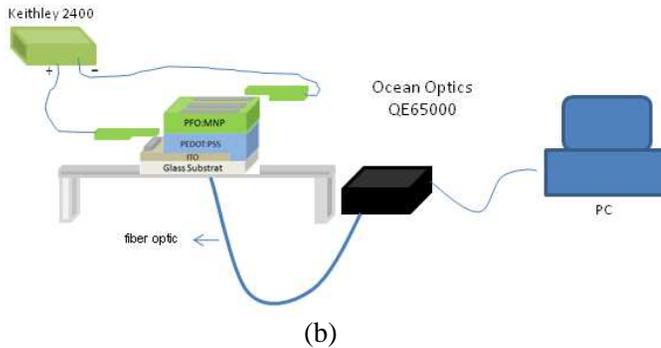are washed with water and acetone to remove unreacted ammonia and

(a)

(b)
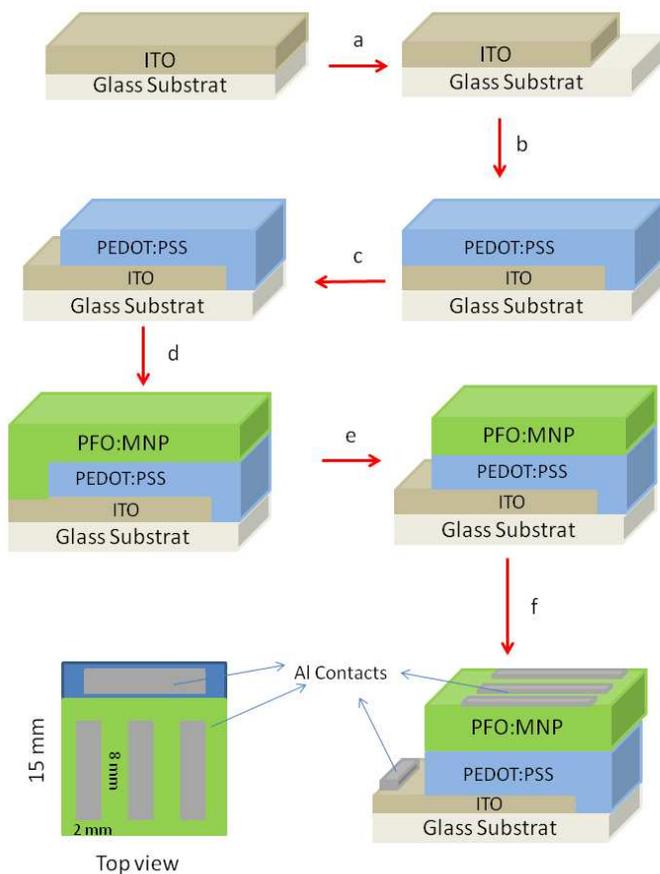
Figure 1. (a) Device fabrication scheme. a — etching a part of ITO coating, b — spin casting of PEDOT:PSS from water dispersion, c — cleaning a part of PEDOT:PSS for anode contact, d — spin coating of active layer (blend of PFO and MNPs), e — cleaning a part of active layer for anode contact, f — evaporation of Al metal electrodes with a mask (PVD technique). (b) Setup for OLED performance test.

oleic acid. Finally the solid material is dried at 70°C for 2 hours. Obtained MNPs are highly soluble in organic solvents such as toluene, hexane, chloroform etc..

2.3. Device Fabrication

The ITO substrates are patterned by a conventional wet-etching process using an acid mixture of HCl and H_2SO_4 as etchant. Patterned ITO glass substrates with a sheet resistance between 10–$12\,\mathrm{square}^{-1}$ are cleaned sequentially with acetone and iso-propanol by ultrasonic bath for 15 minutes, then dried in an oven, and finally treated in an UV/O_3 cleaner. Figure 1(a) shows that the procedure of the device fabrication.

Doping ratio of MNPs are adjusted to be 0.4%, 0.6%, 0.8%, 1% and 2% v/v. PEDOT-PSS ($\sim 40\,\mathrm{nm}$) is spin casted at 4000 rpm for 1 minute on ITO glass, then dried at 120°C for 30 minutes under vacuum. Emissive matrix (MNP doped or pristine PFO) is spin casted at 1200 rpm for 1 minute onto PEDOT:PSS layer. Al cathode (100 nm) is deposited by thermal evaporation through a shadow mask giving an active device area of $0.16\,\mathrm{cm}^2$. Emissive PFO matrix includes 0%, 0.4%, 0.6%, 0.8%, 1% and 2% v/v MNPs. The concentrations of PFO and MNP are 10 mg/ml in chlorobenzene for both materials. All device fabrication and characterization process are carried out under nitrogen atmosphere in a glove box system (MBRAUN-Germany) integrated with device fabrication and characterization units.
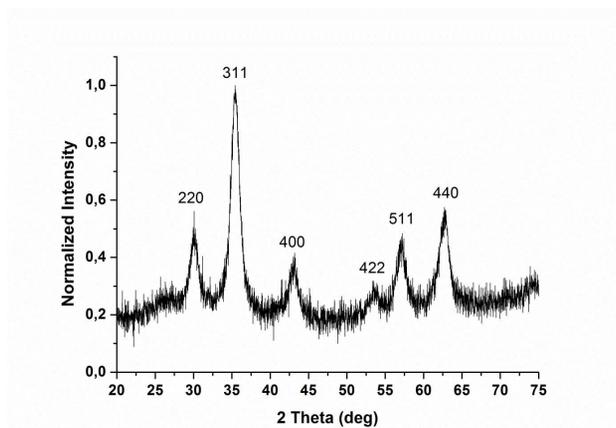
Figure 2. XRD patterns of Fe$_3$O$_4$ MNPs.

3. RESULT AND DISCUSSION

3.1. Synthesis

X-ray diffraction (XRD) pattern of colloidal nanoparticles was recorded using a Bruker Advance D8 XRD (Cu α source with 1.5406 wavelength), in powder mode.

XRD patterns of the Fe$_3$O$_4$ nanostructures demonstrate spinel structure by the characteristic peaks ($2\theta = 30.2°$ (220), $35.5°$ (311), $43.2°$ (400), $53.5°$ (422), $57.1°$ (511), $62.7°$ (440) (PDF No. 01-071-6336), which are consistent with the standard peaks and index for magnetite [39–41]. Broad peaks are due to small size of MNPs. As well known, XRD peaks becomes broadened by decreasing the particle size (Figure 2).

The average crystalline size was calculated from the [311] diffraction peaks by using Scherrers equation as shown below [42]

$$Dc = \frac{0.9 \times \lambda L}{(\cos \theta)}$$

where Dc is the crystalline diameter, L is the half-intensity width of the diffraction peak, λ is the X-ray wavelength and θ is the angle of diffraction. The average particle size is calculated to be 8 nm. Transmission-small angle X ray scattering (T-SAXS) analysis for particle size (not shown here) confirms the particle size.

Figures 3(a)–(b) show TEM images of MNPs. Since magnetic feature lead to aggregation on MNPs some island like feature was observed on TEM image. However the resolution of images allows us

to describe the shape and size of particles. It is clear from Figure 3(b) spinel structures of particles can be easily observed.

Jeol ESR-EMX Plus Electron Spin Resonance (ESR) system was used to show magnetic feature of nanoparticles. Figure 4 shows ESR spectra of MNPs under 0.1 mW applied power at room temperature. It is clear from ESR spectra, symmetric resonance peaks are observed at around 3200 G. Such a symmetric peak shows the purity of MNPs and may be attributed to single type of species [43].

ESR technique is used to show only magnetic feature and purity of MNPs. However detailed analysis of ESR spectra depending on some parameters such as temperature is subject to another study.

Magnetic properties of MNP doped PFO thin films were also investigated by Atomic Force Microscopy (AFM) and Magnetic Force
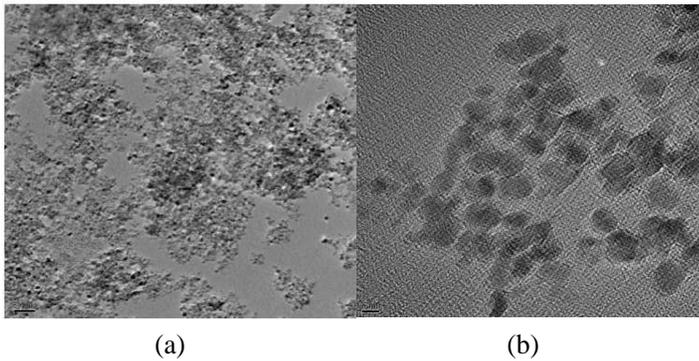

(a)   (b)

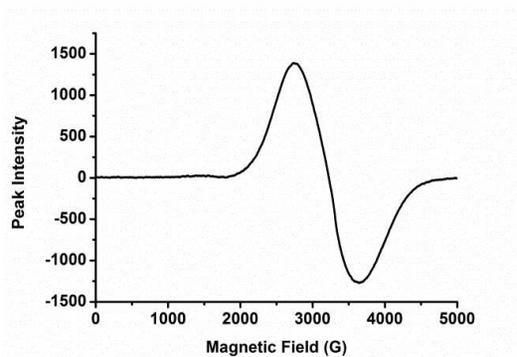**Figure 3.** TEM images of Fe_3O_4 MNPs.
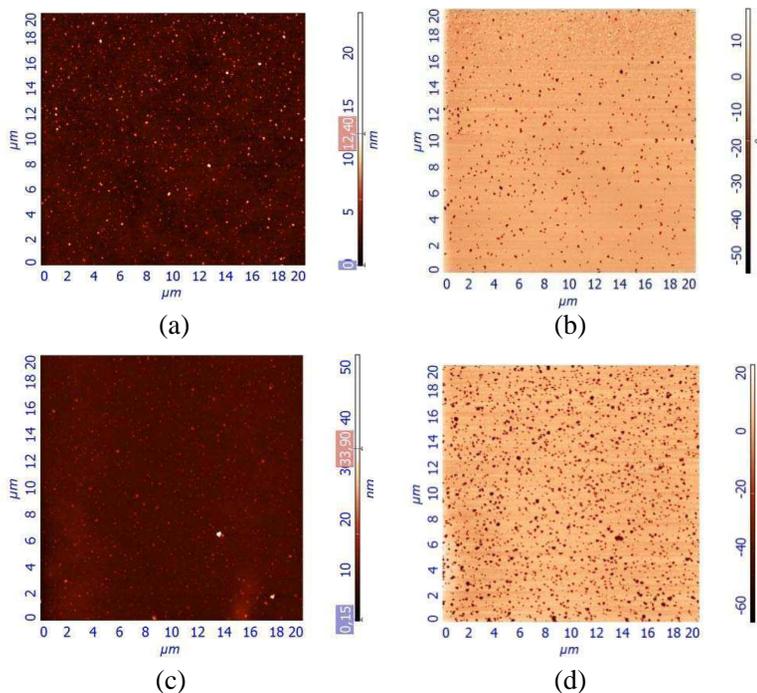

Figure 4. ESR spectra of MNPs.

Figure 5. (a) (c) AFM and (b) (d) MFM images of Fe$_3$O$_4$ MNPs.

Microscopy (MFM). AFM and MFM images of magnetic films were given in Figures 5(a)–(d). Topographic (Figures 4(a) and (c)) and phase (Figures 5(b) and (d)) images give compatible characteristics. The dispersion of MNPs in PFO matrix can be clearly seen in phase image (see Figures 5(b) and (d)) [44]. As well known, magnetic AFM probes are sensitive to magnetic regions of a surface and show strong interaction that result in a threshold in detector response. Thus the magnetic regions on a surface can be clearly observed as we also did. MNPs are appears as dots on phase images in Figures 5(b) and (d).

We have to notice that the homogeneity of dispersion in PFO matrix depends on the spin rate during film preparation. Spin rate below than 1200 rpm causes aggregation of MNPs in polymer matrix (see Figures 5(c) and (d), spin rate is 800 rpm), while better dispersion is observed above than 1200 rpm (see Figures 5(a) and (b), spin rate is 1200 rpm). On the other hand, due to formation of some polymer aggregates, all bulges observed at topographic images do not show magnetic feature at phase images. In comparison Figure 5(a) with Figure 5(c), however at first glance, Figure 5(a) seems like much

rougher than Figure 5(c), but statistic analysis show that the roughness of film spin casted at 1200 rpm (Figure 5(a)) is around 0.44 nm while it is 0.7 nm for the film spin casted at 800 rpm (Figure 5(c)). No doubt that, island-like aggregates are formed by increasing the MNPs concentration in polymer matrix due to magnetic effect. So the performance of MNP doped polymer LEDs strongly depends on both spin rate and concentration of MNPs in polymer matrix.

3.2. Device Performance

Schematic diagram of OLED devices is given in Figure 6. MNP/PFO doping ratios are 0%, 0.4%, 0.6%, 0.8%, 1% and 2% respectively. Pristine PFO device is considered to be reference for comparison.

The electroluminescence measurements were performed with Ocean Optics Q65000 spectrometer. Figure 1(b) shows the scheme of experimental setup for OLED characterization embedded in glove box system. OLED devices were fixed on a homemade sample holder that allows to get electrical contacts from upper side (for Keithley sourcemeter) and a connection from bottom side for fiber optic cable to spectrometer (for Ocean Optics). Luminance measurements were also performed by fixing ADMESY Bronthes-Colorimeter camera instead of fiber optic cable.

Figure 7 shows the current density-voltagecharacteristics of the reference device and 1% MNP doped device. No significant change is observed on turn-on voltage by MNP doping. Sun et al. reported that, CoFe MNPs doped in MEHPPV matrix serve as electron traps and lead to an increased turn-on voltage [36]. They suggested that the electron trapping effect of CoFe MNPs is most probably associated
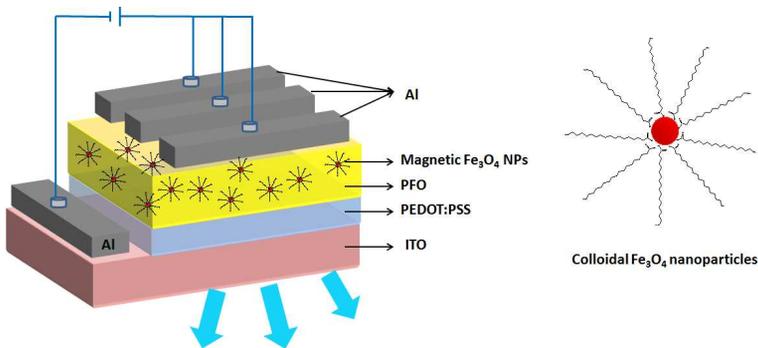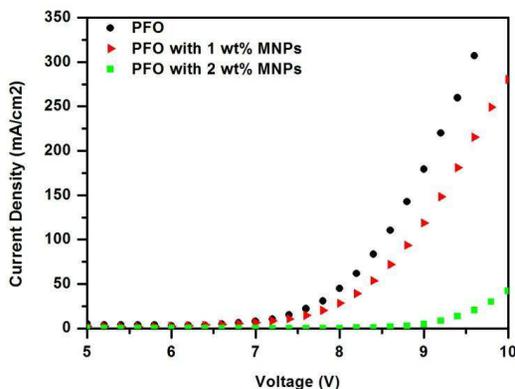

Figure 6. OLED concept.

Figure 7. Current density (mA/cm2) — Voltage (V) characteristics of pristine and 1% MNP doped devices.
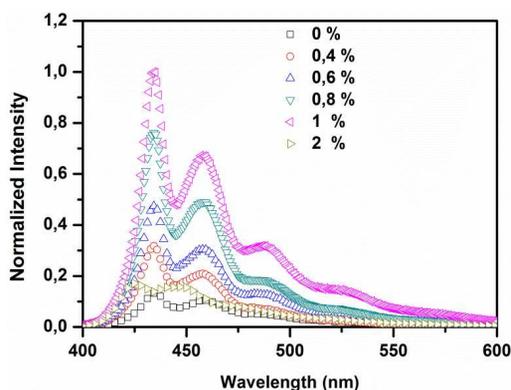

Figure 8. Electroluminescence Spectra of devices depending on different MNP doping ratio varied from 0% (pristine PFO device), 0.4%, 0.6%, 0.8%, 1% and 2% w/v Fe_3O_4, respectively. EL spectra were recorded under 3 mA applied current.

with the oxidized interface between CoFe and MEHPPV [36]. Similar results are observed in case the doping ratio of Fe_3O_4 MNPs is above than 2%. It is also observed that homogeneity of light emitted from device is lost beside the light intensity and lifetime.We attributed that the formation of big Fe_3O_4 aggregates in PFO matrix, which damages film homogenity and prevents current flow due to having insulator capping agent (oleic acids) on their surfaces, lead to an increase of turn-on voltage and a decrease in device performance. MNPs greater
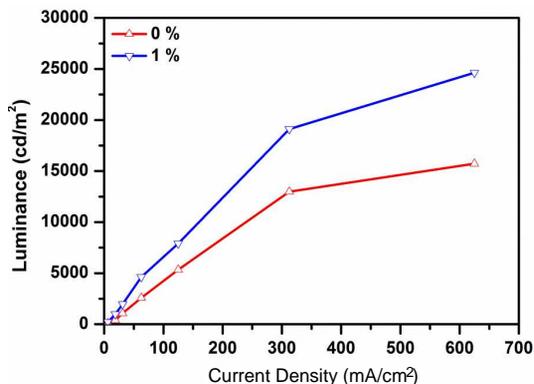
Figure 9. Luminance characteristics of pristine and 1% MNP doped devices depending on current densities.

than 10 nm were also synthesized and used for device fabrication. The results about OLED application with greater MNPs are worthless and not shown here. That is why it is not possible to obtain uniform film with MNPs and also to measure electroluminescence. That is most probably due to aggregation of MNPs in polymer matrix that prevent the formation of uniform film.

Figure 8 shows the EL spectra of pristine PFO and MNP doped devices under 3 mA applied current. The shape of characteristic emission peaks of PFO devices is almost similar with MNP doped devices except for 2% MNP doping. The PFO emission increases by increasing the doping ratio of MNPs up to 1%. Above than 1% doping of MNPs, electroluminescence dramatically decreases beside the change in peak shape is observed. The relative emission peak of 1% MNP doped device 10 fold increase is observed in comparison with pristine PFO device. On the other hand the increase of brightness is observed to be around 60% by 1% MNP doping.

Figure 9 shows luminance characteristics of pristine and 1% MNP doped devices depending on current densities. The increase of luminance is observed to be almost constant above than $600 \, \text{mA/cm}^2$. The luminance of pristine PFO device is $15.000 \, \text{cd/m}^2$ while it is $24.000 \, \text{cd/m}^2$ by 1% MNP doping under $600 \, \text{mA/cm}^2$ applied current. However the increase of luminance is calculated to be around 60% under 600 mA applied current, the average increase is calculated to be around 50% by considering the current between 0–600 mA. The enhancement of luminance may be attributed to the formation of new energy levels. Doping with MNPs causes the formation of

new energy levels in the band gap of host material, which act like traps for holes. These traps balance the hole and electron current, resulting in an enhancement of electroluminescence [36]. It is known that recombination, covered by the fraction of excitons, which are as singlets, is limited to 25%, in case the created excitons ratio of triplet: singlet is 3 : 1 [45]. MNPs doped to emissive layer effect the spin states which resulting in an increase of the singlet exciton fraction and thus recombination process enhances [35, 46].

4. CONCLUSIONS

We report syntheses of colloidal Fe_3O_4 MNPs based on two phase method at low temperatures and their influence on the performance of OLEDs.

Two main conclusions may be emphasized in this study. The first one is facile synthesis of monodisperse colloidal Fe_3O_4 MNPs based on two phase method which is scarce for MNPs. The second one is the considerable luminance enhancement of PFO OLEDs by doping colloidal Fe_3O_4 MNPs which has not been reported for PFO based OLEDs.

ACKNOWLEDGMENT

REFERENCES

1. Li, Y., A. Rizzo, R. Cingolani, and G. Gigli, "Bright white-light-emitting device from ternary nanocrystal composites," *Advanced Materials*, Vol. 18, No. 19, 2545–2548, 2006.

2. Haque, S., S. Koops, N. Tokmoldin, J. Durrant, J. Huang, D. Bradley, and E. Palomares, "A multilayered polymer light-emitting diode using a nanocrystalline metal-oxide film as a charge-injection electrode," *Advanced Materials*, Vol. 19, No. 5, 683–687, 2007.

3. Taberna, P. L., S. Mitra, P. Poizot, P. Simon, and J.-M. Tarascon, "High rate capabilities Fe_3O_4-based Cu nano-architectured electrodes for lithium-ion battery applications," *Nat. Mater.*, Vol. 5, 567–573, 2006.

4. Xu, Z., C. Shen, Y. Hou, H. Gao, and S. Sun, "Oleylamine as both reducing agent and stabilizer in a facile synthesis of magnetite nanoparticles," *Chemistry of Materials*, Vol. 21, 1778–1780, 2009.

5. Zeng, H. and S. Sun, "Syntheses, properties, and potential applications of multicomponent magnetic nanoparticles," *Advanced Functional Materials*, Vol. 18, No. 3, 391–400, 2008.

6. Shi, R., X. Liu, G. Gao, R. Yi, and G. Qiu,, "Large-scale synthesis and characterization of monodisperse Fe_3O_4 nanocrystals," *Journal of Alloys and Compounds*, Vol. 485, 548–553, 2009.

7. Zhang, L., R. He, and H.-C. Gu, "Oleic acid coating on the monodisperse magnetite nanoparticles," *Applied Surface Science*, Vol. 253 2611–2617, 2006.

8. Bronstein, L. M., X. Huang, J. Retrum, A. Schmucker, M. Pink, B. D. Stein, and B. Dragnea, "Influence of iron oleate complex structure on iron oxide nanoparticle formation," *Chemistry of Materials*, Vol. 19, No. 15, 3624–3632, 2007.

9. Sun, J., S. Zhou, P. Hou, Y. Yang, J. Weng, X. Li, and M. Li, "Synthesis and characterization of biocompatible Fe_3O_4 nanoparticles," *Journal of Biomedical Materials Research A*, Vol. 80, No. 2, 333–341, 2007.

10. Mai Hoa L. T., T. T. Dung, T. M. Danh, N. H. Duc, and D. M. Chien, "Preparation and characterization of magnetic nanoparticles coated with polyethylene glycol," *Journal of Physics: Conference Series*, Vol. 187, 12048, 2009.

11. Xuan, S., L. Hao, W. Jiang, X. Gong, Y. Hu, and Z. Chen, "Preparation of water-soluble magnetite nanocrystals through hydrothermal approach," *Journal of Magnetism and Magnetic Materials*, Vol. 308, 210–213, 2007.

12. Lartigue, L., K. Oumzil, Y. Guari, J. Larionova, C. Guerin, J.-L. Montero, V. Barragan-Montero, C. Sangregorio, A. Caneschi, C. Innocenti, T. Kalaivani, P. Arosio, and A. Lascialfari, "Water-soluble rhamnose-coated Fe_3O_4 nanoparticles," *Organic Letters*, Vol. 11, No. 14, 2992–2995, 2009.

13. Pan, D., S. Jiang, L. An, and B. Jiang, "Controllable synthesis of highly luminescent and monodisperse CdS nanocrystals by a two-phase approach under mild conditions," *Advanced Materials*, Vol. 16, No. 12, 982–985, 2004.

14. Dallas, P., A. Bourlinos, D. Niarchos, and D. Petridis, "Synthesis of tunable sized capped magnetic iron oxide nanoparticles highly soluble in organic solvents," *Journal of Materials Science*, Vol. 42, 4996–5002, 2007.

15. Hui, C., C. Shen, T. Yang, L. Bao, J. Tian, H. Ding, C. Li, and H.-J. Gao, "Large-scale Fe_3O_4 nanoparticles soluble in water synthesized by a facile method," *The Journal of Physical Chemistry C*, Vol. 112, 11336–11339, 2008.

16. Kalinowski, J., M. Cocchi, D. Virgili, P. Di Marco, and V. Fattori, "Magnetic field effects on emission and current in Alq_3-based electroluminescent diodes," *Chemical Physics Letters*, Vol. 380, No. 5, 710–715, 2003.

17. Gomez, J. A., F. Nüesch, L. Zuppiroli, and C. F. O. Graeff, "Magnetic field effects on the conductivity of organic bipolar and unipolar devices at room temperature," *Synthetic Metals*, Vol. 160, Nos. 3–4, 317–319, 2010.

18. Nguyen, T. D., Y. Sheng, J. Rybicki, G. Veeraraghavan, and M. Wohlgenannt, "Magnetoresistance in pi-conjugated organic sandwich devices with varying hyperfine and spin-orbit coupling strengths, and varying dopant concentrations," *Journal of Materials Chemistry*, Vol. 17, 1995–2001, 2007.

19. Ding, B. F., Y. Yao, Z. Y. Sun, C. Q. Wu, X. D. Gao, Z. J. Wang, X. M. Ding, W. C. H. Choy, and X. Y. Hou, "Magnetic field effects on the electroluminescence of organic light emitting devices: A tool to indicate the carrier mobility," *Applied Physics Letters*, Vol. 97, 163302–163304, 2010.

20. Shimada, T. *Organic Light Emitting Diode — Material, Process and Devices*, 311–322, InTech, 2011.

21. Ohmori, Y., H. Kajii, T. Sawatani, H. Ueta, and K. Yoshino, "Enhancement of electroluminescence utilizing confined energy transfer for red light emission Autore," *Thin Solid Films*, Vol. 393, 407–411, 2001.

22. Zhang, D.-D., J. Feng, Y.-F. Liu, Y.-Q. Zhong, Y. Bai, Y. Jin, G.-H. Xie, Q. Xue, Y. Zhao, S.-Y. Liu, and H.-B. Sun, "Enhanced hole injection in organic light-emitting devices by using Fe_3O_4 as an anodic buffer layer," *Applied Physics Letters*, Vol. 94, 223303–223306, 2009.

23. Scherf, U. and E. J. W. List, "Semiconducting polyfluorenes-towards reliable structureCproperty relationships," *Advanced Materials*, Vol. 14, No. 7, 477–487, 2002.

24. Neher, D., "Polyfluorene homopolymers: Conjugated liquid-crystalline polymers for bright blue emission and polarized electroluminescence," *Macromolecular Rapid Communications*, Vol. 22, No. 17, 1365–1385, 2001.

25. Yu, W.-L., J. Pei, W. Huang, and A. J. Heeger, "Spiro-functionalized polyfluorene derivatives as blue light-emitting

materials," *Advanced Materials*, Vol. 12, No. 11, 828–831, 2000.

26. Grell, M., D. D. C. Bradley, M. Inbasekaran, and E. P. Woo, "A glass-forming conjugated main-chain liquid crystal polymer for polarized electroluminescence applications," *Advanced Materials*, Vol. 9, No. 10, 798–802, 1997.

27. Pei, Q. and Y. Yang, "Efficient photoluminescence and electroluminescence from a soluble polyfluorene," *Journal of the American Chemical Society*, Vol. 118, 7416–7417, 1996.

28. Rathnayake, H., A. Cirpan, Z. Delen, P. Lahti, and F. Karasz, "Optimizing OLED efficacy of 2,7-diconjugated 9,9-dialkylfluorenes by variation of periphery substitution and conjugation length," *Advanced Functional Materials*, Vol. 17, 115–122, 2007.

29. Craig, M. R., M. M. de Kok, J. W. Hofstraat, A. P. H. J. Schenning, and E. W. Meijer, "Improving color purity and stability in a blue emitting polyfluorene by monomer purification," *Journal of Materials Chemistry*, Vol. 13, 2861–2862, 2003.

30. Jenekhe, S. A. and J. A. Osaheni, "Excimers and exciplexes of conjugated polymers," *Science*, Vol. 265, 765–768, 1994.

31. Gong, X., P. K. Iyer, D. Moses, G. C. Bazan, A. J. Heeger, and S. S. Xiao, "Stabilized blue emission from polyfluorene-based light-emitting diodes: Elimination of fluorenone defects," *Advanced Functional Materials*, Vol. 13, 325–330, 2003.

32. Becker, K., J. Lupton, J. Feldmann, B. Nehls, F. Galbrecht, D. Gao, and U. Scherf, "On-chain fluorenone defect emission from single polyfluorene molecules in the absence of intermolecular interactions," *Advanced Functional Materials*, Vol. 16, 364–370, 2006.

33. Niedermeir, U., "Magnetic field effect in organic light emitting diodes," Ph.D. Thesis, Technishe Universitat Darmstadt, 2010.

34. Francis, T. L., O. Mermer, G. Veeraraghavan, and M. Wohlgenannt, "Large magnetoresistance at room temperature in semiconducting polymer sandwich devices," *New Journal of Physics*, Vol. 6, 185, 2004.

35. Itskos, G., E. Harbord, S. K. Clowes, E. Clarke, L. F. Cohen, R. Murray, P. Van Dorpe, and W. Van Roy, "Oblique Hanle measurements of InAs/GaAs quantum dot spin-light emitting diodes," *Applied Physics Letters*, Vol. 88, 22113–22114, 2006.

36. Sun, C.-J., Y. Wu, Z. Xu, B. Hu, J. Bai, J.-P. Wang, and J. Shen, "Enhancement of quantum efficiency of organic light emitting devices by doping magnetic nanoparticles," *Applied*

Physics Letters, Vol. 90, 232110–232113, 2007.

37. Kumar P., H. Kumar, S. Chand, S. C. Jain, V. Kumar, V. Kumar, R. P. Pant, and R. P. Tandon, "Effect of CoFe magnetic nanoparticles on the hole transport in poly (2-methoxy, 5-(2-ethylhexiloxy) 1,4-phenylenevinylene)," *Journal of Physics D: Applied Physics*, Vol. 41, 185104, 2008.

38. Zhang, W., Y. Xu, H. Wang, C. Xu, and S. Yang, "Fe_3O_4 nanoparticles induced magnetic field effect on efficiency enhancement of P3HT: PCBM bulk heterojunction polymer solar cells," *Solar Energy Materials and Solar Cells*, Vol. 95, 2880–2885, 2011.

39. Lee, J., T. Isobe, and M. Senna, "Preparation of ultrafine Fe_3O_4 particles by precipitation in the presence of PVA at high pH," *Journal of Colloid and Interface Science*, Vol. 177, 490–494, 1996.

40. Zhou, Z. H., J. Wang, X. Liu, and H. S. O. Chan, "Synthesis of Fe_3O_4 nanoparticles from emulsions," *Journal of Materials Chemistry*, Vol. 11, 1704–1709, 2001.

41. Si, S., A. Kotal, T. K. Mandal, S. Giri, H. Nakamura, and T. Kohara, "Size-controlled synthesis of magnetite nanoparticles in the presence of polyelectrolytes," *Chemistry of Materials*, Vol. 16, 3489–3496, 2004.

42. Scherrer, P., "Gottinger Nachrichten," *Gesell*, Vol. 2, 98, 1918.

43. Koseoglu, Y., "Effect of surfactant coating on magnetic properties of Fe_3O_4 nanoparticles: ESR study," *Journal of Magnetism and Magnetic Materials*, Vol. 300, e327–e330, 2006.

44. Leo, G., Y. Chushkin, S. Luby, E. Majkova, I. Kostic, M. Ulmeanu, A. Luches, M. Giersig, and M. Hilgendorff, "Ordering of free-standing Co nanoparticles," *Materials Science and Engineering: C*, Vol. 23 949–952, 2003.

45. Friend, R. H., R. W. Gymer, A. B. Holmes, J. H. Burroughes, R. N. Marks, C. Taliani, D. D. C. Bradley, D. A. D. Santos, J. L. Bredas, M. Logdlund, and W. R. Salaneck, "Electroluminescence in conjugated polymers," *Nature*, Vol. 397, 121–128, 1999.

46. Chen, C.-H. and H.-F. Meng, "Enhancement of singlet exciton formation ratio in electroluminescent conjugated polymers by magnetic doping," *Physical Review B*, Vol. 68, 1–9, 2003.